Effect of Lifting Body on Multirotor Flight Performance

Yoonjae Lee* and Jack W. Langelaan†
Department of Aerospace Engineering, The Pennsylvania State University

Many Unmanned Aerial Vehicles (UAVs) designed for urban delivery missions are equipped with Vertical Take-Off and Landing (VTOL) capabilities, primarily to minimize drag during flight. However, the absence of adequate aerodynamic considerations pertaining to lift potential can limit the overall flight efficiency in terms of range and endurance. This study endeavors to comprehensively analyze the impact of incorporating a lifting body on multirotor flight performance. The analysis encompasses a meticulous selection process for the airfoil, an in-depth examination of its aerodynamic attributes encompassing lift, drag, and thrust properties, as well as an evaluation of stationary hover performance during flight. The chosen lifting body configuration comprises a cargo pod paired with the MH-84 flying wing airfoil, with thrust serving as a proxy for power requirements. The results demonstrate that an airfoil mounting angle of 20 degrees exhibits remarkable efficiency gains, leading to up to an 84 percent reduction in energy consumption during cruise while maintaining a satisfactory stationary hover performance even under challenging windy conditions.

Nomenclature

α	=	Airfoil angle of attack
θ	=	Rotor pitch angle
γ	=	Flight path angle in x-y direction
ξ	=	Airfoil mounting angle
m	=	Mass
c	=	Airfoil cord length
S	=	Airfoil surface area
V	=	Airspeed
g	=	Gravitational acceleration
l_{ac}	=	Distance between center of mass to aerodynamic center
l_1, l_2	=	Length: center of mass to rotor 1 and rotor 2 respectively
T_1	=	Thrust by front rotor
T_2	=	Thrust by back rotor
T	=	Total thrust
T_d	=	Rotor 1 and rotor 2 thrust difference

I. Introduction

Multirotor Unmanned Aerial Vehicles (UAVs, colloquially referred to as drones) have been widely used in both the consumer market for entertainment, photography or videography, and the industrial sector for inspection and surveying, as well as certain demonstration projects for package delivery. As laws governing the operation of drones and other unmanned air vehicles evolve to enable flying beyond visual line of sight (BVLOS), package delivery and other long-range missions will become increasingly common. This implies that efficient cruise will become an increasingly crucial component of drone operations. UAVs designed for the delivery missions in the urban area are capable of Vertical Take-Off and Landing (VTOL) while minimizing drag-enabling operation from the urban landing pods envisioned for VTOL vehicles. This aerodynamic consideration allows multirotor to perform stationary hover, but the absence of incorporating a lifting body reduces the potential aerodynamic advantage during a cruise.

*Schreyer Honors College Undergraduate Student, Department of Aerospace Engineering, 229 Hammond Building, University Park, PA 16802. AIAA Student Member
†Professor of Aerospace Engineering, 229 Hammond Building, University Park, PA 16802. AIAA Associate Fellow

Multirotors remain a valuable arrangement because they are mechanically simple, easily controlled, and may have redundant actuation depending on the number of rotors. They are, however, not very aerodynamic, with a high drag coefficient and extensive rotor-rotor and rotor-body contact. Variants such as the biplane quadrotor tailsitter (citation) attempt to mitigate the aerodynamic cost by shifting to a forward flight mode where the main lift force is provided by the wings. Multirotors with tilting rotors add mechanical complexity (a tilting system) to increase cruise efficiency.

For instance, Fixed-wing Quadrotor (FWQ) configuration takes advantage of aerodynamics by attaching a pusher propeller and wing. Rather than supplying power to the main rotors that give upward and forward forces during a cruise, inducing lift that covers rotors' upward force reduces power consumption into the main quadrotors. It generates forward force solely by the additional pusher rotor and flies like a regular aircraft.

Tilt-rotor and tilt-wing quadrotor also attach wings onto the quadrotor to take an aerodynamic advantage of the wings. Unlike FWQ, tilting mechanisms tilts the main rotors, generating forward force. Because the attached wing, rotors, and tilting mechanism do not support hover performance, these additional components unnecessarily increase the overall weight during hover. Considering that the power requirements during hover increase by the third-half power of its weight, these non-functioning additional weights significantly increase the energy required to hover. Furthermore, UAVs with a tilting mechanism add more mechanical complexity and require an additional transitional flight controller.

Here we describe a lifting body multirotor. It seeks to keep the mechanical simplicity of a multirotor (i.e. all control is managed via varying rotor speeds) while improved aerodynamic efficiency by exploiting by lift and reduced drag. Here a low order analysis of cruise performance and hover performance in gusty conditions is presented to determine a good rotor/body incidence to balance both phases of flight.

Tail-sitter also uses a wing to enhance the cruise performance but reduces the added weight, eliminates mechanical complexity, and removes additional controller mode. It also flies like a regular aircraft during the cruise by horizontally leaning the aircraft and utilizing all rotors to function as a pusher rotor. This configuration seems to eliminate most problems noted earlier while preserving lifting body benefits. However, during hover, the vertically standing wing causes the vehicle to be more affected by wind and reduces stationary hover performance. Modifying the vertical airfoil mounting angle to a slant angle (which becomes lifting body quadrotor) would reduce the wind disturbance's aerodynamic effect during hover while partially maintaining the benefit of lift during the cruise. Therefore lifting the body quadrotor leads to a trade-off between flight efficiency during the cruise and stationary hover: This research explores the airfoil mounting angle that balances energy efficiency during forward and stationary flight and finds the accommodated efficiency in flight range and endurance.

We will discuss a multirotor with a lifting body in this section. It aims to maintain the mechanical simplicity of a multirotor (all control is accomplished by adjusting rotor speeds) while increasing aerodynamic efficiency through the use of lift and reducing drag. The purpose of this article is to offer a low-order study of cruise and hover performance under windy circumstances in order to establish the optimal rotor/body incidence for balancing both phases of flight.

The rest of this paper is arranged in the following manner. Section II discusses the integration of a lifting body and a multirotor; Section III discusses a hypothetical design; Section IV discusses cruise performance; Section V discusses hover stationkeeping; finally Section VI concludes.

II. Integrating Body Aerodynamics into Multirotor Design

Airfoil choice based on the wing-body enables reducing drag caused by excess skin and parts, enlarge volume inside the wing, and generating a more stable lift. Then, the OpenVSP program rendered a 3D model of the quadrotor considering the design characteristics mentioned in introduction and computed an aerodynamic coefficients of the lifting body for every two degrees intervals in angles of attack. Matlab program is then used to compute the required data such as lift, drag and thrust for several velocity increment. 12 state-space system matrices equation of motion were developed to demonstrate the wing's lift and drag aerodynamic effects. Simulink simulated the vehicle dynamics with the equation of motion mentioned and controlled hover flight with the Linear–quadratic regulator–cost value driven by Bryson's rule.

A. Coordinate Frames

Figure 1 shows the placement of the variables and frame used in the study. NED frame is used where n axis points forward (cruise) direction and d axis points downward direction. e axis points out of the page if referencing the diagram shown in figure 1. However, its axis is not considered nor shown in the diagram to simply its dynamics into 2D motion. The rotor closer to the airfoil tailing edge is labeled as the first rotor and the rotor closer to the airfoil leading edge is labeled as the second rotor. Therefore, the length of CG to the first rotor is l_r1 and CG to the second rotor is l_r2. Likewise, T_1 and T_2 represents thrust from the rotor from the first and the second rotor. l_ac represents the length between

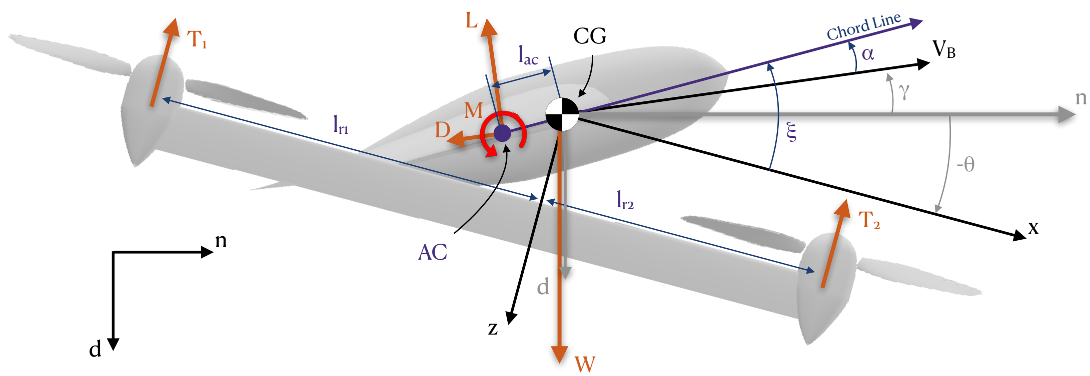

Fig. 1 Terms shown in a diagram

CG and the aerodynamic center where its length can be adjusted to reduce the thrust difference. L and D represents lift and drag forces, and M represents airfoil moments.

Angle terms are measured as positive in a counterclockwise direction from the n axis. In this diagram, for example, value of α, ξ and γ are positive, but θ is negative since x reference is rotated clockwise from the n axis. With these sign convention and the consideration of the aerodynamic properties, the equation of motion of the vehicle is as follows:

Aforementioned forces and moment are represented with a red and thick arrows and length force terms are not to scale, but they are well

B. Derivation of Equations of Motion

$$\dot{n} = u\cos\theta + w\sin\theta \tag{1}$$

$$\dot{d} = -u\sin\theta + w\cos\theta \tag{2}$$

$$\dot{\theta} = q \tag{3}$$

$$\ddot{n} = \frac{1}{m}[-(T_1 + T_2)\sin\theta - L\sin\gamma - D\cos\gamma] \tag{4}$$

$$\ddot{d} = \frac{1}{m}[W - (T_1 + T_2)\cos\theta - L\cos\gamma - D\sin\gamma] \tag{5}$$

$$\ddot{\theta} = \frac{1}{I_{ac}}[-T_1(l_1 - l_{ac}) + T_2(l_1 + l_{ac}) - W\bar{l}_{ac}\cos(\xi - (-\theta))] \tag{6}$$

Where θ is the angle between the horizontal reference to the rotor, γ is the flight path angle, α is the airfoil angle of attack, ξ is the rotor mounting angle, T_1 and T_2 are front and back rotor thrust, m is total mass of the vehicle, l_1 is the length between center of mass to rotor length, and l_{ac} is the length between aerodynamic center and the center of mass. Also, C_L and C_D each represents lift and drag coefficient. Therefore, applied forces are

$$W = mg \quad , \quad L = \frac{1}{2}\rho V^2 S C_L(\alpha) \quad , \quad D = \frac{1}{2}\rho V^2 S C_D(\alpha)$$

Equation 4, 5 and 6 represents the motion along N and E direction and pitching moment. The study looks for the analysis during the straight flight, therefore, the flight path angle, γ, is set to zero. With this consideration, equation 4 and 5 becomes:

$$\ddot{n} = -\frac{(T_1 + T_2)}{m}\sin\theta - \frac{D}{m} \tag{7}$$

$$\ddot{d} = \frac{W}{m} - \frac{(T_1 + T_2)}{m}\cos\theta - \frac{L}{m} \tag{8}$$

C. Steady-state Flight Performance

Setting the static equilibrium, $\ddot{n}$, $\ddot{n}$ and $\ddot{\theta}$ becomes zero, and the lift (L), drag (D) and moment (M) depends on other variables: airspeed (V) and angles of attack (α). Knowing that θ, γ, ξ and α relationship is $\xi - \alpha - \gamma = \theta$, the following equations of motion can be driven:

$$-(T_1 + T_2)\sin\theta = D \tag{9}$$

$$-(T_1 + T_2)\cos\theta = L - W \tag{10}$$

Combining equation 9, 10 and 6, the total thrust (T), trust difference (T_d) and angles of attack (α) can be expressed as:

$$(T_1 + T_2)^2 = (L(V,\alpha) - W)^2 + D^2(V,\alpha) \tag{11}$$

$$T_d = T_1 - T_2 = \frac{(l_{ac}L - M(V,\alpha))}{l_r} \tag{12}$$

$$\alpha = \arctan\left(\frac{-D(V,\alpha) - W\sin\gamma}{-L(V,\alpha) + W\cos\gamma}\right) + \xi \tag{13}$$

Then, Newton Raphson is applied to equation 13 and get equation 14. This is done to find the force static equilibrium on the vehicle. With the consideration of equation 11, 12 and 14, Matlab program repeated the computation with the accuracy setting of 0.01 degrees for α.

$$\alpha_i = \arctan\left(\frac{-D(V,\alpha) - W\sin\gamma}{-L(V,\alpha) + W\cos\gamma}\right) + \xi + \alpha_{i+1} \tag{14}$$

III. Design of a Lifting Body Multirotor

A lifting body based on a flying wing is described as an example. Notably, this constrains the choice of airfoil, assuming that the vehicle is adjusted to be trimmable and stable in forward flight. The configuration of the lifting body will be compared to that of a non-lifting body which was modelled as a spherical center body as shown in the figure **??**. The body has been intended to be statically stable, with an acceptable position of the CG and AC, and to be trimmable. Aerodynamic characteristics such as lift coefficient, drag coefficient, and pitch moment coefficient at cruise flight angles of attack. Angles of attack ranging from −10 to 45 degrees were determined using the aerodynamic analysis program VSPAero. In Figure 4, the coefficients are displayed as a function of the angle of attack. Body that is incapable of raising A non-lifting body with comparable measurements will be used to compare performance. (including three perspectives)

A. Typical Non-lifting Body

An airframe with a spherical body mimics the aerodynamic effect of the typical quadrotor. This configuration works as the standard design and will be compared with the lifting body airframe. Figure 1 below is a threeview of the spherical body quadrotor. The size of the sphere were chosen based on the survey of the ratio between typical cumercial quadrotor's body and overall quadrotor airframe.

B. Airfoil Choice

According to theoretical considerations by xxx, flying wings are presented as the most aerodynamically efficient design arrangement for a fixed-wing aircraft (cite). This efficiency is done by carefully choosing the most suitable airfoil profile, resulting in the lowest drag. It would also have high structural efficiency. With its characteristic of absence of a clear distinctive section between the wing and the main body, more cargo space can be obtained and result in high fuel efficiency. The main consideration of the use of flying wing is the controllability of the yaw control due to the absence

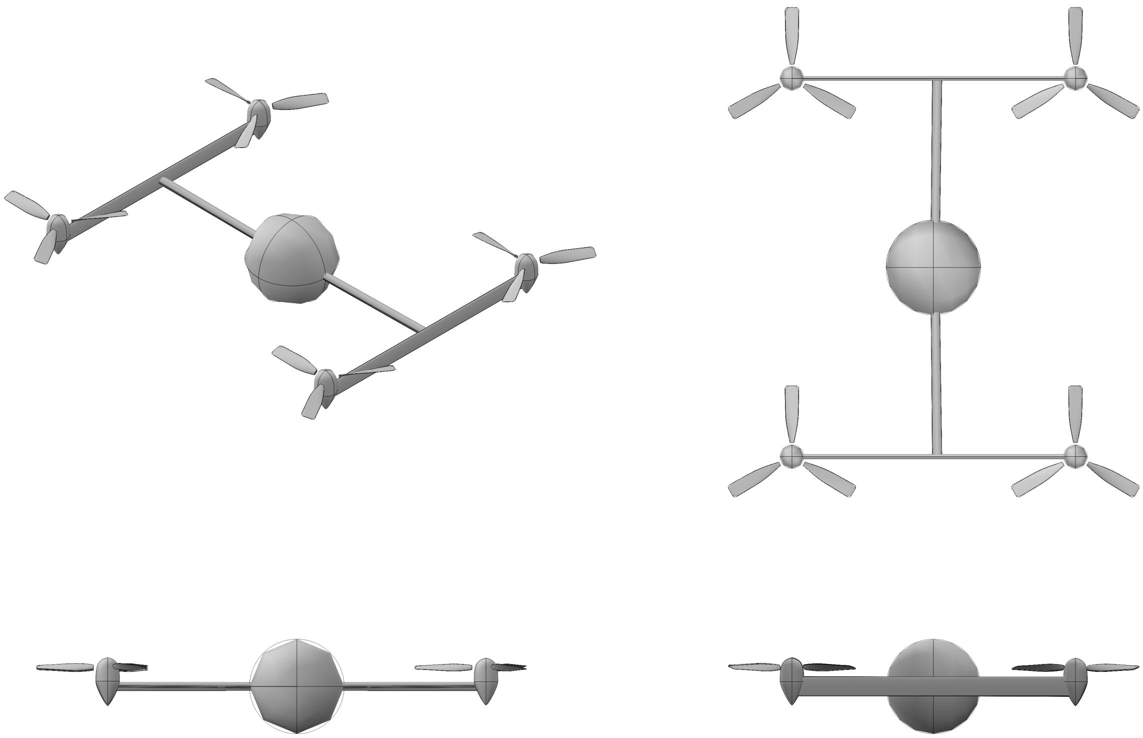

Fig. 2 Aircraft with sphere body that represents the typical cumercial quadrotor airframe

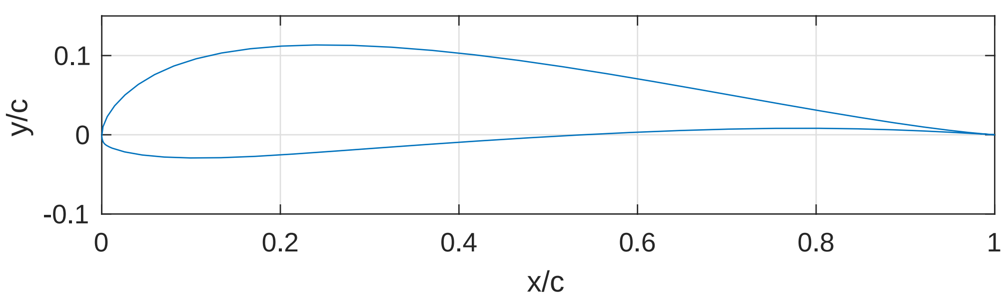

Fig. 3 MH 84 meets the desirable aerodynamic requirement for lifting bodies

of the vertical stabilizer. There are many ways of overcome this problem; in the later section which explains the design consideration would give a detail demonstration of overcoming the overall rotational control.

The most suitable airfoil is chosen based on the aerodynamic properties such as Lift drag and moment coefficient. There were several airfoil choices within flying wings, but MH 84 (cite airfoil tool) were chosen for the following reasons:

1) Enough Lift at zero angles of attack: This characteristic allows the aircraft to generate enough lift during cruise and stay away from generating negative lift during hover performance.
2) High lift to drag ratio to obtain the most aerodynamic efficiency: When the aircraft reaches the force equilibrium, lift equals weight and thrust equals drag. With high lift to drag ratio, less drag is obtained with the same lift force. Less drag leads to less thrust, therefore fuel can be saved.
3) Consistent moment coefficient during cruising airspeed: As briefly mentioned above, flying wing suffer from the pitch and yaw control. Fortunately, the characteristic of quadrotor which has rotor separation from the center of mass and AC well overcome the pitch control. In this configuration, the consistence moment better suit the needs of yaw control.

C. Aerodynamics Coefficient for Cruising range

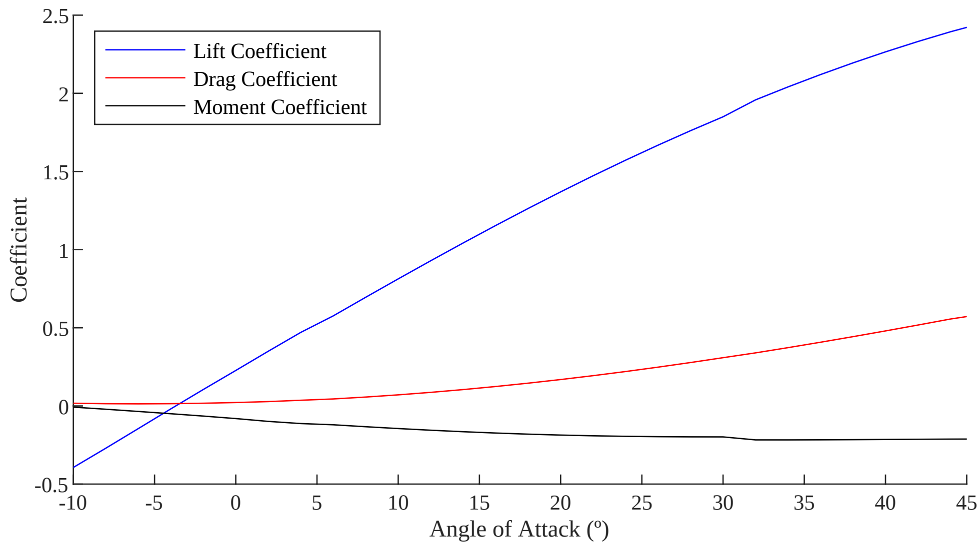

Fig. 4 Aerodynamic coefficient characteristic with a consideration of the body (from -25 to 45 degrees)

Figure 4 shows the aerodynamic characteristic considers both airfoil and body. Rather then applying the aerodynamic coefficient data from the original course, OpenVSP program aerodynamic simulation is used to find demonstrated data. This is mainly to consider the aerodynamic effect of the whole lifting body which includes the cargo pod attached to the wing. This also allow to check the aerodynamic effect in a flight test in practice. Reynolds number of 6e+6, which is closed to the Reynolds number during cruise (20 to 30 m/s).

OpenVSP is also used to design overall look of the aircraft, the figure 5 shows the overall design of the vehicle. As mentioned in introduction, the design contains the flying wings on top of the regular quadrotor design. The center of mass of the cargo pod is aligned with the center of mass of rotor frame and aerodynamic center is slightly placed behind center of mass due to the trim-ability.

[Assumptions in progress] (Aerodynamics effects of body (rotor and its frame) is negligible) (CM AC location and $l_a c$)

D. Yaw Control

Note that the rotors that controls yaw during cruise are tilted 15 degrees better control the yaw. As explained in the introduction section, the wing-body aircraft significantly lack in yaw control due to the absence of horizontal stabilizer. In this study, the aircraft controls yaw by giving more power to certain rotors and generate the reaction torque. However, during cruise, yaw could also be applied by the thrust imbalance relative to the center of mass. Considering that the moment is based on the force and moment arm, slightly tilting the rotors outwards results increasing the overall moment arm, thus, increasing the yaw control.

IV. Effect of rotor incidence on performance

Explained by xxx and xxx, the mounting angle is a term in fixed-wing airfraft, which is the angle between the chord line of the wing and a reference axis along the fuselage [citate]. The equation of motion analyzed the relationship between the airfoil mounting angle and the energy required to cruise. The optimization does not need to consider the motions in sideway or yaw, so the equation of motions only considered 2D motion: forward, upward, downward, and pitch.

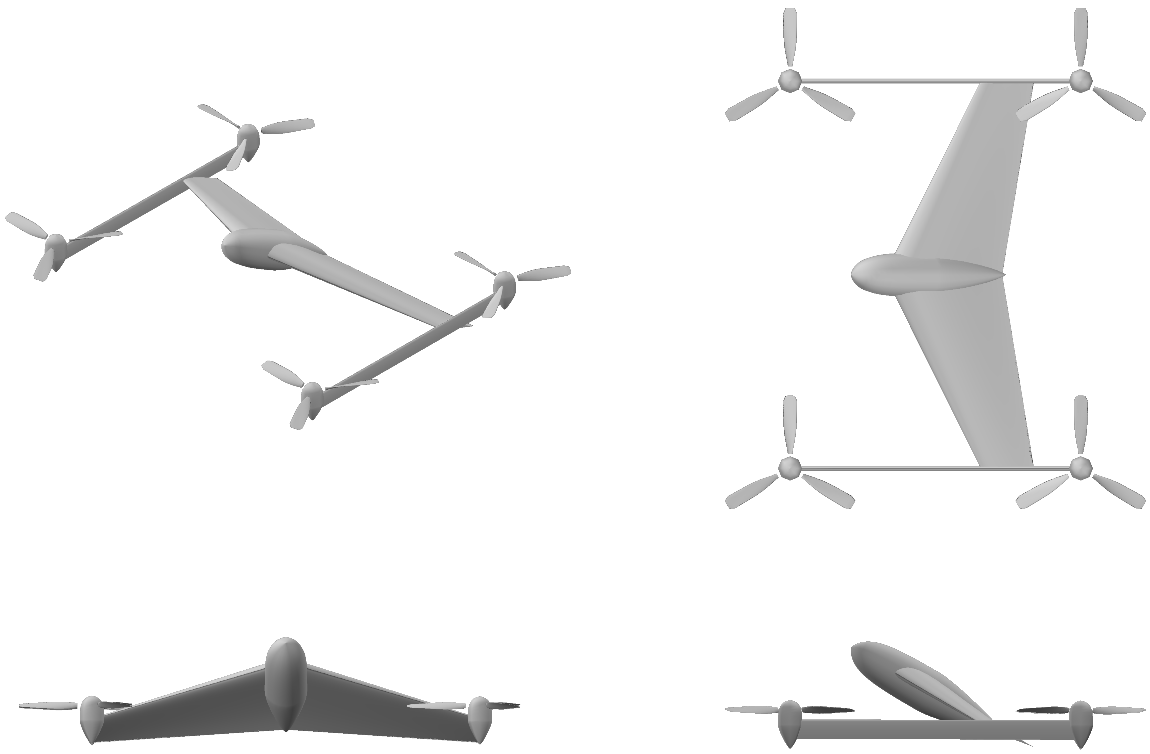

Fig. 5 Overall Vehicle Design Contains Flying Wings on top of the Typical Quadrotor

A. 2D Equation of Motion

Computation for several steady states were also repeated for all intermediate mounting angles until 40 degrees, and intermediate airspeed until of 30 m/s. Spherical body and 90 degrees mounting angle were also considered to get the reference data explained in introduction. For each two degrees increment of rotor angle, Matlab ploted the required angle of attack (Fig. 6) for a given airspeed. Moreover, the plot of lift (Fig. 7) and drag (Fig. 8) generated by the aerodynamic effect were also determined based on the angle of attack computation.

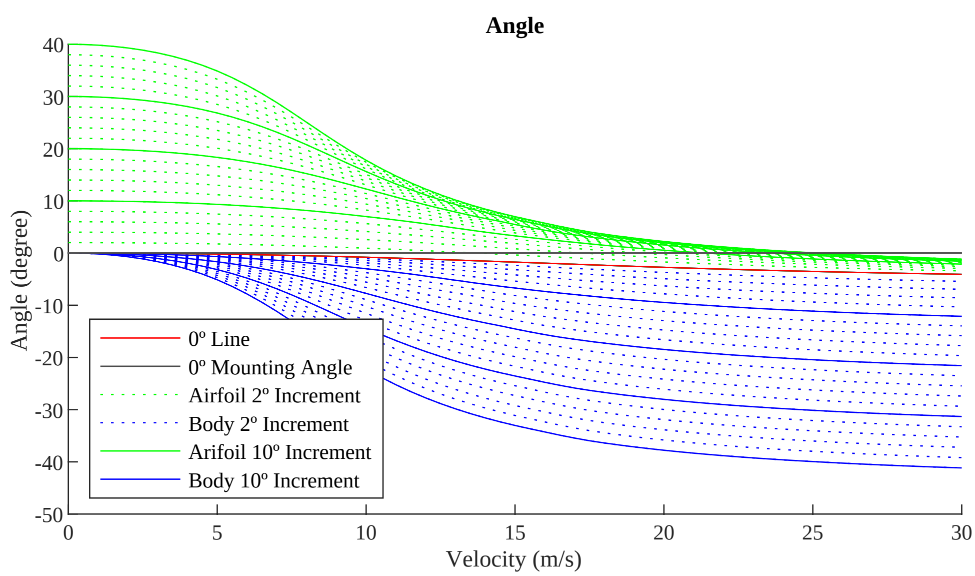

Fig. 6 Zero angle of attack at 25 m/s airspeed regardless of mounting angle choices

B. Lift, Drag and Angle of Attack

From Fig. 6, shows that as the vehicel gains in speed, the vehicle pitches more to make more significantly larger thrust. This is done by applying thrust in forward as well and pitching the body forward. Compared to the spherical body, the aids of wing's lift allows the thrust to significantly reduce its upward direction and make more forward direction. This leads the aircraft to pitch more with a wing attachment. This effect gets more significant as the mounting angle increases. More importantly, with MH 84 flying wing airfoil, figure shows that the airfoil has the zero angle of attack at airspeed of 23 m/s regardless of mounting angle.

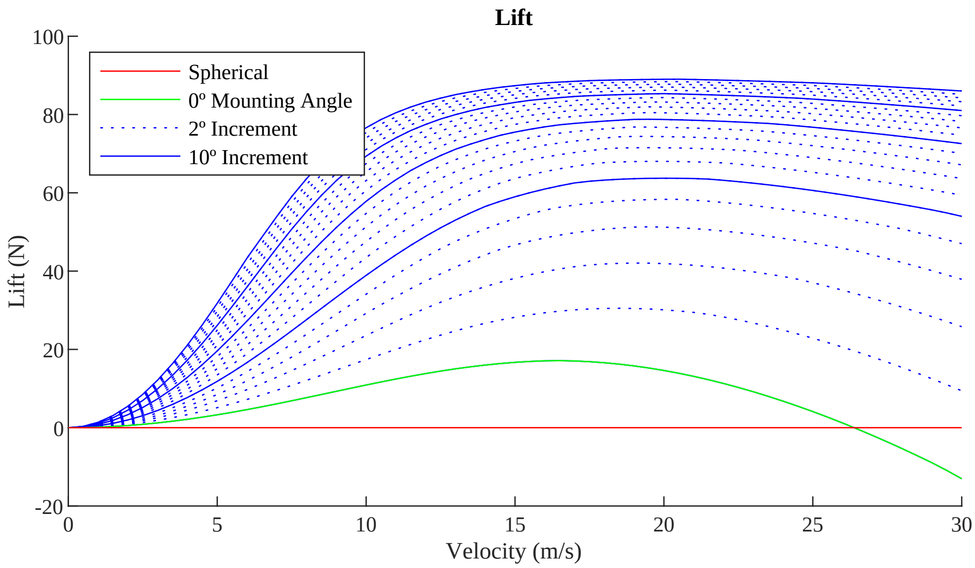

Fig. 7 Lift gets gradually larger along with airfoil mounting angle

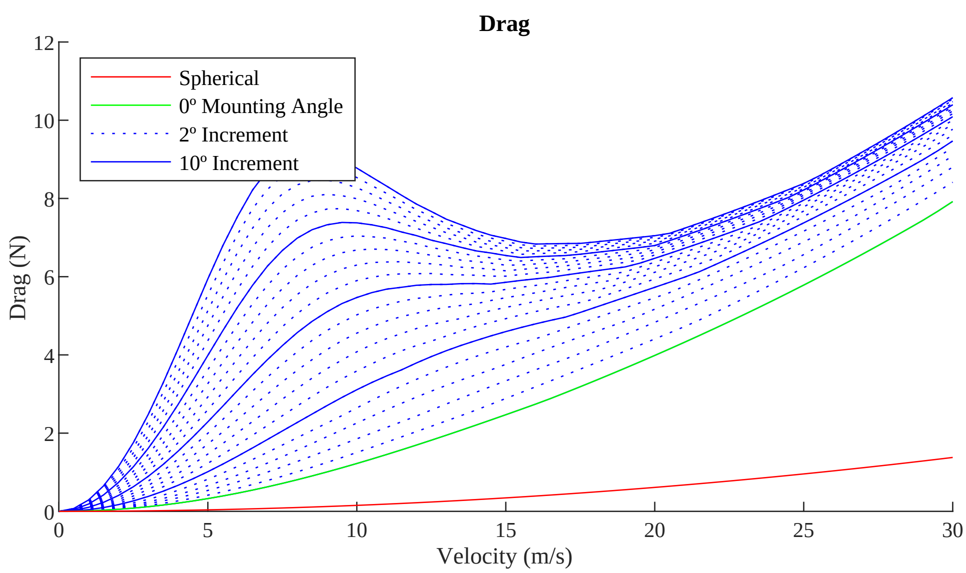

Fig. 8 Drag gets significantly lower within 10 to 25 m/s region

Figure 7 and 8 shows that both lift and drag gets significantly larger with an attachment of flying wing airfoil. The increasing trend is large at the lowing mounting angle and gradually gets smaller as the mounting angle increases. In other words, the aerodynamic effect by the airfoil attachment is significant even just with an attachment and its effect get lower and lower as the mounting angle increases.

Figure 8 also clearly shows the overall effect of drag on vehicle. At lower speed (until 10m/s), the induced drag governs the most of the drag due to the high angles of attack. After 10 m/s, the induced drag gets significantly lower due to the increase in angle of attack, then the the drag curve follows quadratic relationship with airspeed.

C. Power Requirement

Through plotting lift, drag and angle of attack, the study is looking for the thrust requirement due to consideration of thrust as a proxy for power. To get the most range, finding a point of the minimum thrust relative to the velocity is desirable. This is done by finding the minimum slope of the thrust to velocity ratio. Figure 9 shows the thrust requirement for a certain velocity depending on the airfoil mounting angle.

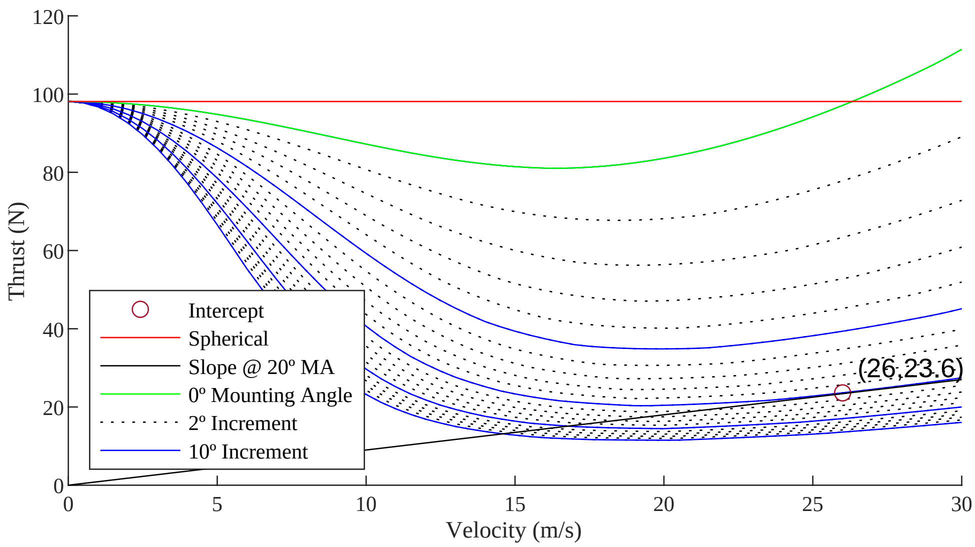

Fig. 9 Thrust

As expected, the higher mounting angle seems to require the lease thrust for the given velocity. Choice of 90º mounting angle would do the most adequate in terms of the fuel efficiency, however, it would be the same configuration as the tail sitter which has a disadvantage of stationary hover performance in wind blow.

As shown by figure 7 and 8, the advantage of airfoil do not follow linearly with a mounting angle increment. Their significance decreases with a constant mounting angle increment, and this trend applies to the thrust requirement as well.

After 20º mounting angle the thrust requirement do not seem to increase as much compared to the mounting angle up to 20º. Requiring only 24.1 percent of energy compared to the non-lifting body is already significant improvement in terms of flight efficiency. Further increasing the mounting angle will provide more efficient flight, however due to the consideration of the stationary hover performance, 20º mounting angle might be the ideal choice.

The difference in thrust is also considered to avoid the individual thrust being negative thrust. Considering the equation 12, change in l_{ac} determined the the thrust required for the front and back rotor, however does not give any effect on the other terms such as angle, lift, drag and total thrust. This is because l_{ac} term appears in equation 12.

Therefore, l_{ac} is set manually to find the least difference in individual thrust. Considering that 20º mounting angle at 26 m/s airspeed seems to be the ideal choice, the l_{ac} were chosen manually to minimize the thrust difference.

Figure 12 shows the thrust requirement for each rotor. This plot is based on l_{ac} of 0.16 meters, which is about 10 percent of length between two rotors (l_1), and is important to show that individual thrust do not pass the zero thrust-not generating negative thrust.

V. Hover Performance Simulation

Before AIAA can print or publish any paper, the copyright information must be completed in the submission system. Failure to complete the electronic form correctly could result in your paper not being published. The following fields must be completed:

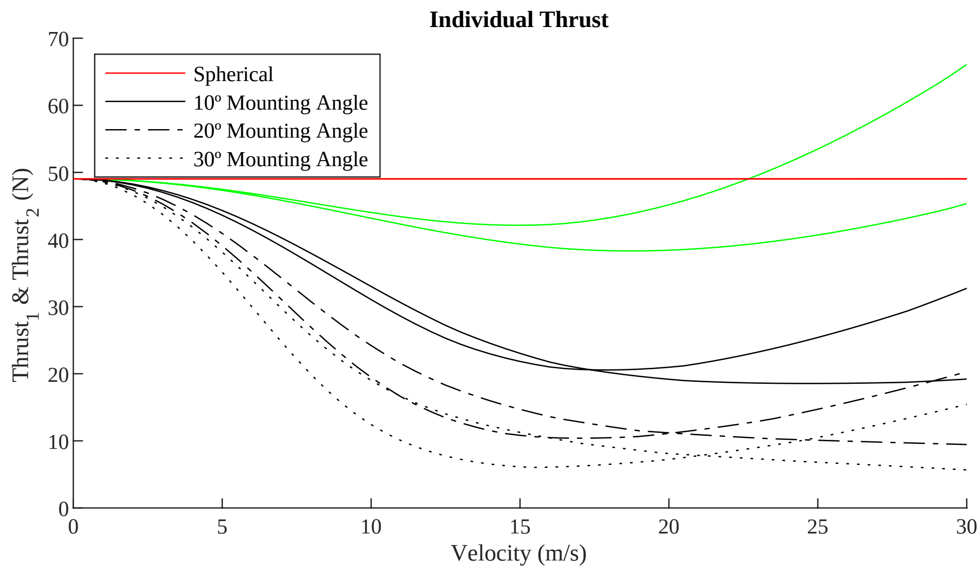

Fig. 10 Thrust

A. Wind Speed Settlement

Since the simulation tries to depict the blow characteristic, the wind blow consist of the main wind speed and perturbation blow speed. The main blow is settled by the regulation settled by Federal Aviation Administration: the main wind speed would be based on its effect on the vehicle during the take off and landing. The maximum wind blow should not exceed the vehicle cruising speed during take off. This way, the vehicle can take off vertically and obtain safe take off. The wind perturbation should also be restricted by the stationary hover capacity of the vehicle. The vehicle must stay within 1.5 times the length of its airframe or its landing pod diameter. Setting the airframe and landing pod diameter to be 1 meter, the wind perturbation caused by the wind blow should be the speed that vehicle would not change it's position more than 1.5 meters. XXX stated that the characteristic and magnitude of the wind perturbation depends on the average wind blow speed (xxx, 20xx). The wind blow characteristic would be based on xxx's description.

B. Aircraft Perturbation

The equation of motion then extended to 3D motion 12 state-space system matrices considering the wing's lift and drag aerodynamic effects when modeling quadrotor dynamics. Simulink simulated the vehicle dynamics with the equation of motion mentioned above and controlled hover flight with the Linear–quadratic regulator–cost value driven by Bryson's rule. In a simulation, a hovering vehicle with every 10 degrees increment (0 to 90 degrees) in rotor angles and a spherical object were placed to a wind blow up to 15 meters per second which is large enough than the real-world stressful wind condition.

The simulation shows that the main wind speed governs the overall vehicle position: xx m/s for spherical body, xx m/s for xx degree mounting angle wing body and xx m/s for tail-wing. Moreover, the vehicle perturbation is also caused by the horizontal wind perturbation as expected, however its perturbation seems to do lesser effect on the the overall vehicle position. This would mean that the main wind blow is the governing wind blow speed and maximum wind blow should be determine by the main wind blow. In terms of the perturbation of the vehicle in wind blow of 3 m/s, spherical body perturbs xx meters, xx degree wing body perturbs xx meters and tail-wing perturbs xx meters.

VI. Conclusion

The simulation results unequivocally showcase the advantages of employing a lifting body with the MH-84 flying wing airfoil in multirotor UAV design. This configuration not only demonstrates remarkable energy savings, reaching an impressive percentage at a cruising speed of 15 meters per second but also exhibits reduced susceptibility to wind disturbances during hover. When compared to the substantial perturbation observed in a 90-degree mounting angle tail-sitter, the 20-degree mounting angle flying wing configuration maintains hover perturbation at a tolerable level. It is worth noting that this configuration may exhibit somewhat diminished stationary hover performance in contrast to a non-lifting spherical body. Nevertheless, the undeniable benefits in terms of energy efficiency make the adoption of the lifting body configuration a compelling choice.

Furthermore, our findings indicate that a 15-degree mounting angle appears to be the most optimal configuration for the MH-84 flying wing airfoil. This specific angle not only yields significant gains in flight efficiency but also ensures adequate stationary hover performance. To conclusively validate and corroborate these outcomes, it is imperative to acquire experimental data, bridging the gap between theory and simulation. Such empirical evidence will offer crucial insights into the real-world behavior of the lifting body configuration, thereby solidifying its merit in multirotor UAV design and operation.

Acknowledgments

I would like to express my heartfelt gratitude to Dr. Jack W. Langelaan for his exceptional research guidance, which has been instrumental in my journey of acquiring profound knowledge and advancing this project. It has been a privilege and a source of great pleasure to develop a higher level of proficiency within the research program under his mentorship. I also extend my sincere appreciation to the Pennsylvania State University Schreyer Honors College for providing me with comprehensive and professional training in research methodologies.

As I look ahead, my commitment to the pursuit of scientific research remains unwavering. I am enthusiastic about continuing this endeavor in the coming years, where I aim to further refine my research skills and cultivate the critical thinking abilities that are indispensable for driving scientific breakthroughs. It is my fervent hope that my research endeavors in the domain of Unmanned Aerial Vehicles and related fields will garner the recognition they deserve. I wholeheartedly dedicate myself to advancing aerospace technology and contributing to the ever-evolving landscape of scientific discovery.

References